Process Zone Length Scales

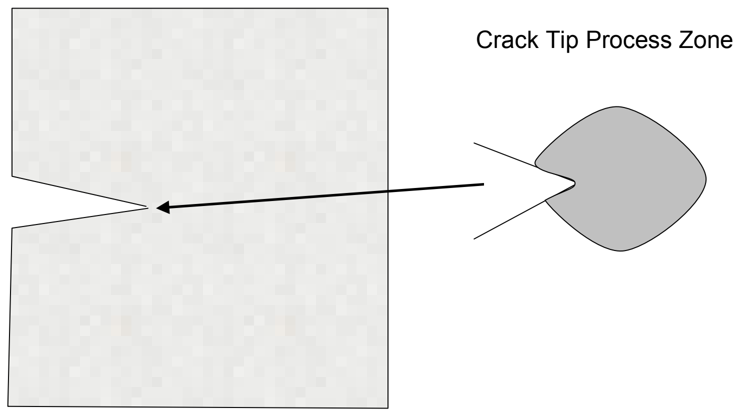

- Plastic zone ahead of a crack tip is crucial to material failure
- Length scales within this zone control blunting
- Toughness depends on crack tip blunting
- Options → DNS or Multiresolution Continuum

Optimization with Multiscale Localization for Materials Toughness and Strength Design

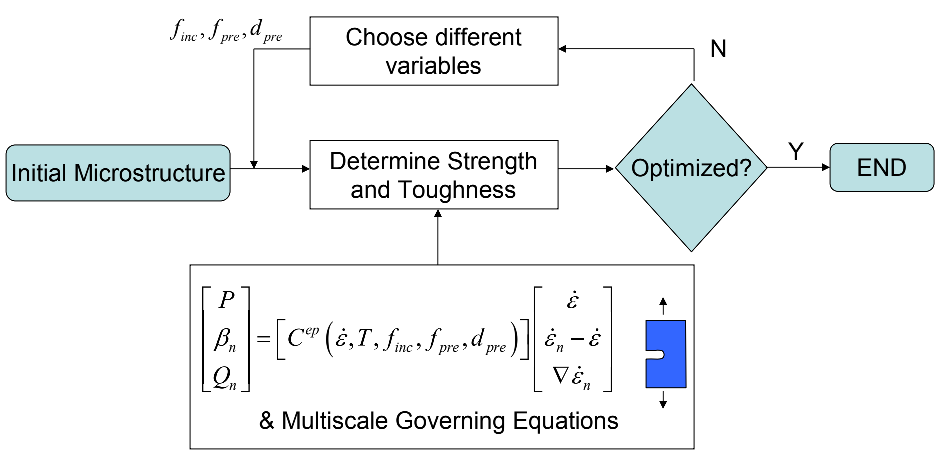

Scales are inter-related through the internal state variables which describe the evolving microstructure

Validation Experiment and Comparison

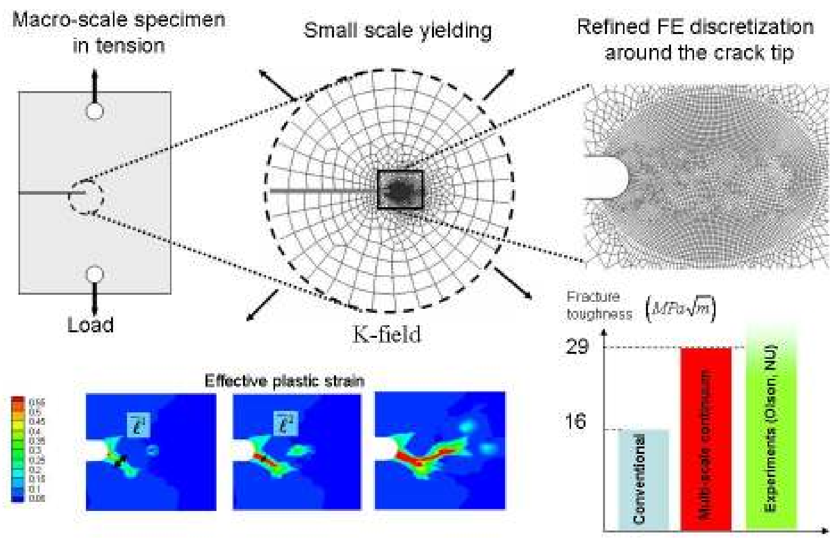

Multiscale Trends in Fracture Toughness

The fracture toughness can be investigated in terms of design parameters. The curves are produced by varying one parameter and keeping the others constant

$$K_{Ic} = K_{Ic}\left(\sigma_{y0}, \frac{|\mathbf{C}^1|}{|\mathbf{C}|}, f^p, \sigma^s, \sigma^p\right)$$

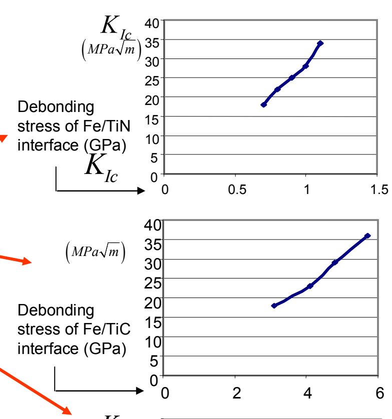

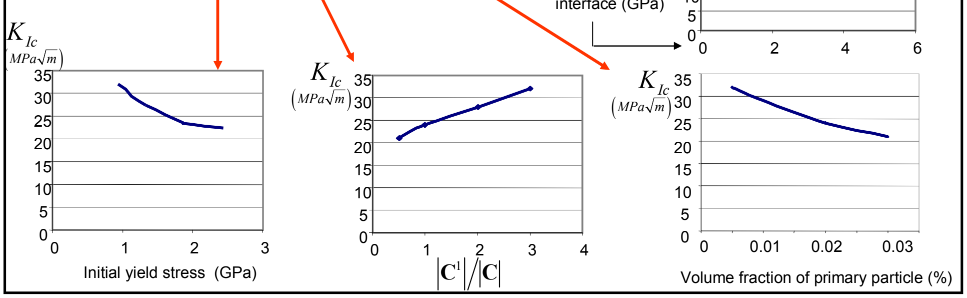

Inhomogeneous Deformation: WC-Co

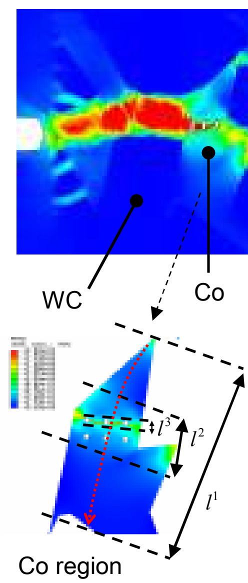

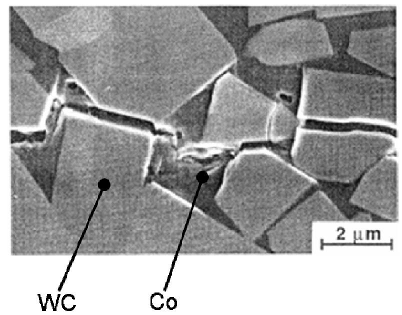

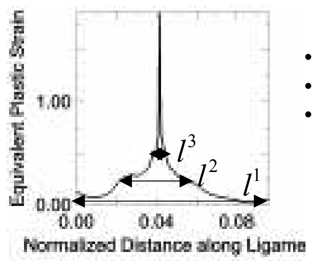

- Size of Cobalt Ligament l^1
- Dislocation hardening l^2
- Void Coalescence l^3

Length Scales of Failure by DNS

- Capture crack tip blunting to predict correct fracture behavior
- Plastic deformation localizes sequentially at four scales

(1) Over the cobalt ligament l^1

(2) Scale related to dislocations in the cobalt l^2 $\quad g_\alpha = (1-k_T\vartheta)g_0\left(\left(1+\frac{\gamma_\alpha}{\gamma_0}\right)^n + k_y d_{Co}^{-1/2}\right)$ $\quad d_{Co}$ grain size

(3) Between neighboring nucleated voids l^3

(4) Within the ligaments between neighboring voids l^4

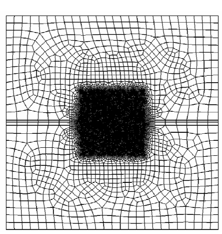

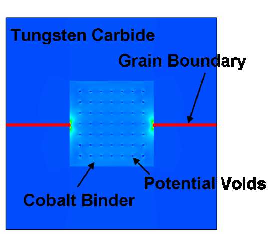

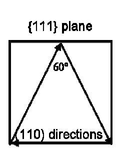

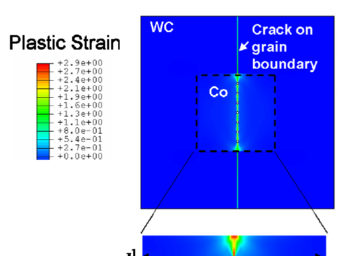

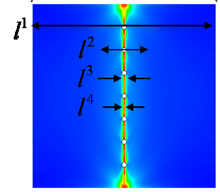

Undeformed configuration

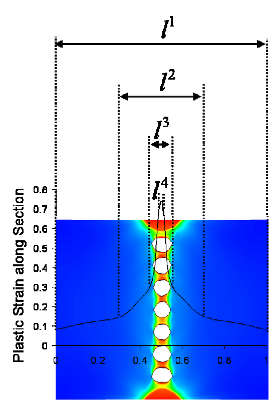

Deformed configuration

Conventional Continuum Approach (Void)

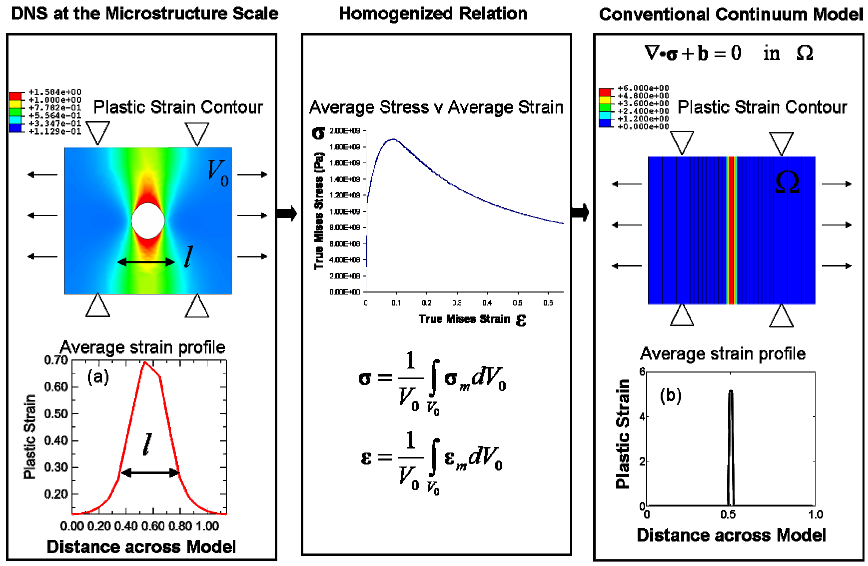

Multiscale Continuum Approach (Void)

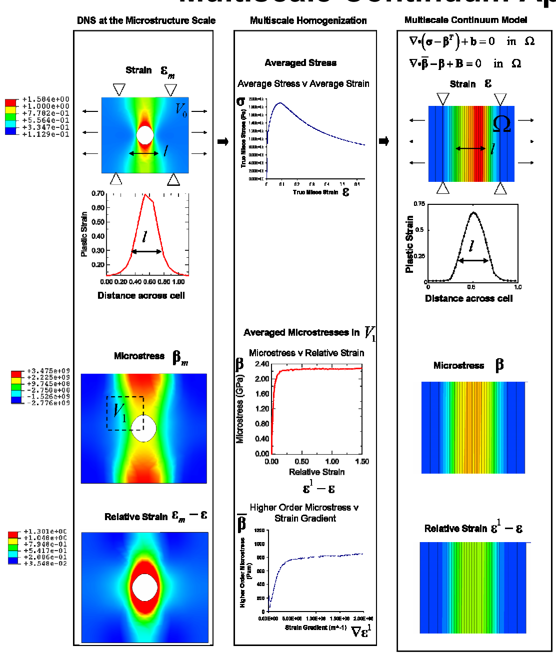

EXTRA microscale constitutive relations are required to describe the microstress and microstrain response

The length scale of localization is embedded through the EXTRA constitutive relationships

Computing Microstresses via DNS

- Power Equivalence Equation used
- Microstresses represent a resistance to heterogeneous deformation at a scale

$$\boldsymbol{\sigma}_m : \mathbf{L}_m^T - \boldsymbol{\sigma} : \mathbf{L}^T = \boldsymbol{\beta}_m : \left(\mathbf{L}_m^T - \mathbf{L}^T \right)$$

- Plot of the evolving microstress in the microstructure

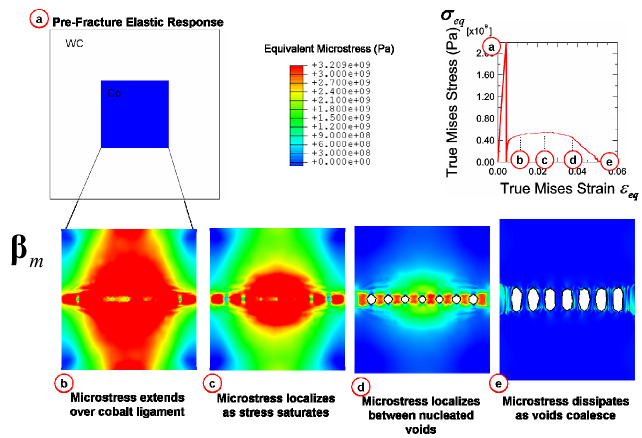

$$\boldsymbol{\sigma} = \frac{1}{V_0} \int_{V_0} \boldsymbol{\sigma}_m dV_0$$

$$\boldsymbol{\varepsilon} = \frac{1}{V_0} \int_{V_0} \boldsymbol{\varepsilon}_m^T dV_0$$

Continuum Microstresses

- We have computed the field $\boldsymbol{\beta}_m$ using $\boldsymbol{\sigma}_m : \mathbf{L}_m^T - \boldsymbol{\sigma} : \mathbf{L}^T = \boldsymbol{\beta}_m : \left(\mathbf{L}_m^T - \mathbf{L}^T \right)$
- The continuum microstresses are given by

$$\boldsymbol{\beta}^n = \frac{1}{V_n} \int_{V_n} \boldsymbol{\beta}_m dV_n \qquad \overline{\boldsymbol{\beta}}^n = \frac{1}{V_n} \int_{V_n} \boldsymbol{\beta}_m \mathbf{y} dV_n$$

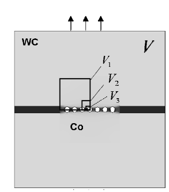

Defining the averaging volumes at each scale

- Assumed velocity gradient varies linearly in averaging volume
- Use this to define averaging volume sizes in heterogeneously deforming region

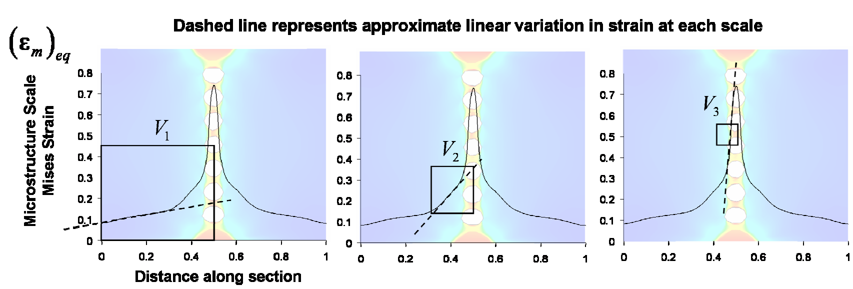

Continuum Microstresses

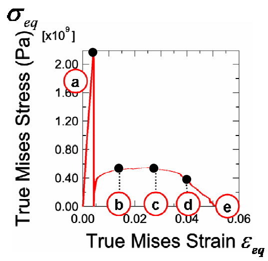

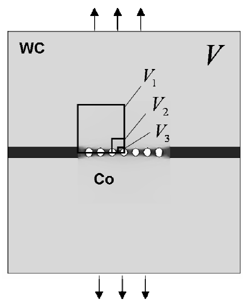

$$\sigma_{eq} = \frac{1}{V}\int_V (\sigma_m)_{eq}\, dV \quad \beta^1_{eq} = \frac{1}{V_1}\int_{V_1} (\beta_m)_{eq}\, dV \quad \beta^2_{eq} = \frac{1}{V_2}\int_{V_2} (\beta_m)_{eq}\, dV \quad \beta^3_{eq} = \frac{1}{V_3}\int_{V_3} (\beta_m)_{eq}\, dV$$

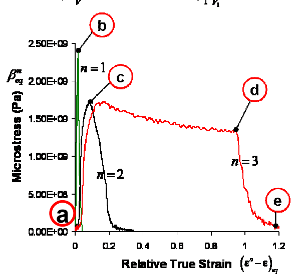

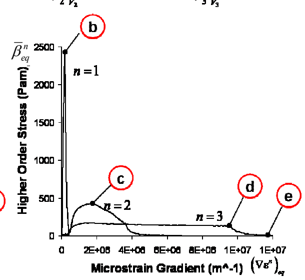

- (a) Carbide fracture; start of inhomogeneous deformation
- Three clear scales of localization in this material
- Three averaging volumes
- Three continuum microstresses

$$\dot{\boldsymbol{\beta}}^n\left(\mathbf{L}^n - \mathbf{L}\right), \dot{\bar{\boldsymbol{\beta}}}^n\left(\mathbf{G}^n\right)$$

- Three instability points which coincide with microstress failure (b), (c), (d)
- These instability points describe microstructure level events
- (b) Stress saturation in the Cobalt
- (c) Nucleation of microvoids
- (d) Coalescence of microvoids

Continuum Microstresses

Material Instability Points

Microstresses

Underlying Physics

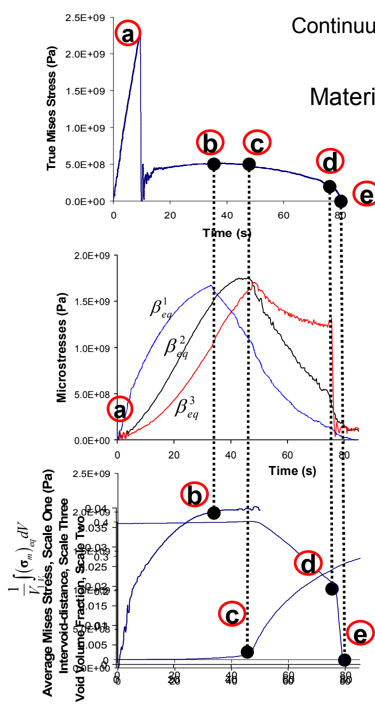

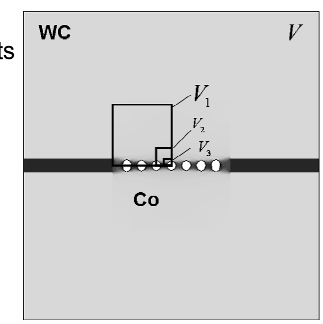

$$\beta^1_{eq} = \frac{1}{V_1}\int_{V_1} (\beta_m)_{eq}\, dV$$

$$\beta^2_{eq} = \frac{1}{V_2}\int_{V_2} (\beta_m)_{eq}\, dV$$

$$\beta^3_{eq} = \frac{1}{V_3}\int_{V_3} (\beta_m)_{eq}\, dV$$

b Saturation stress, β^1_{eq} collapses

c Void Nucleation, β^2_{eq} collapses

d Void Coalescence, β^3_{eq} collapses

e Final failure, all microstress are zero

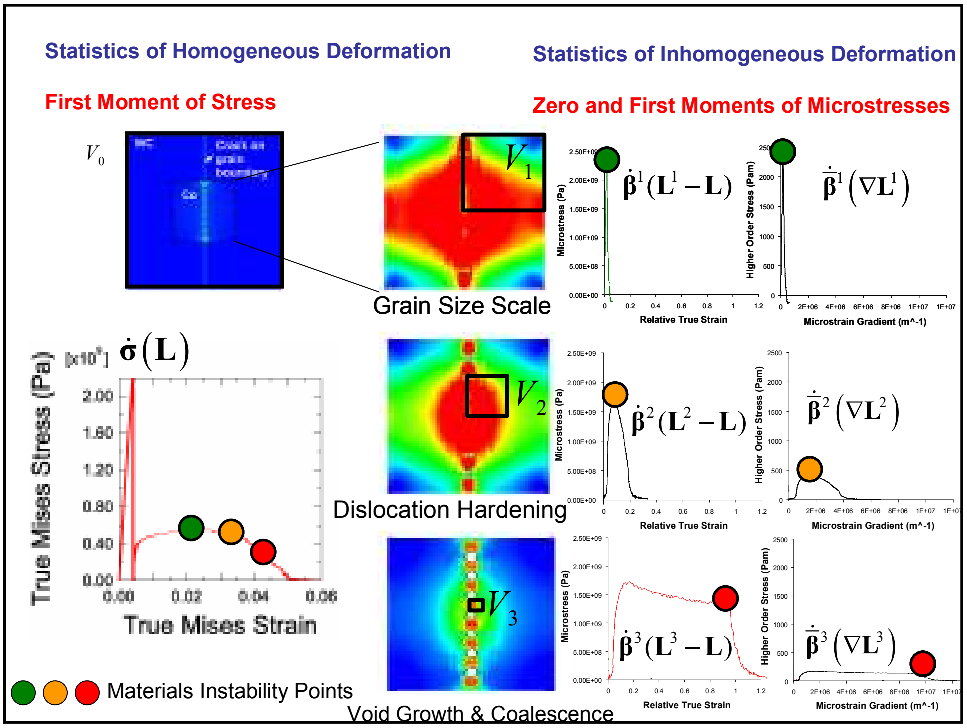

Multiscale Fracture Toughness (WC-Co)

Each constitutive relation is defined we can solve the multiscale governing equations

$$\boldsymbol{\sigma}, \boldsymbol{\beta}^n, \bar{\boldsymbol{\beta}}^n$$

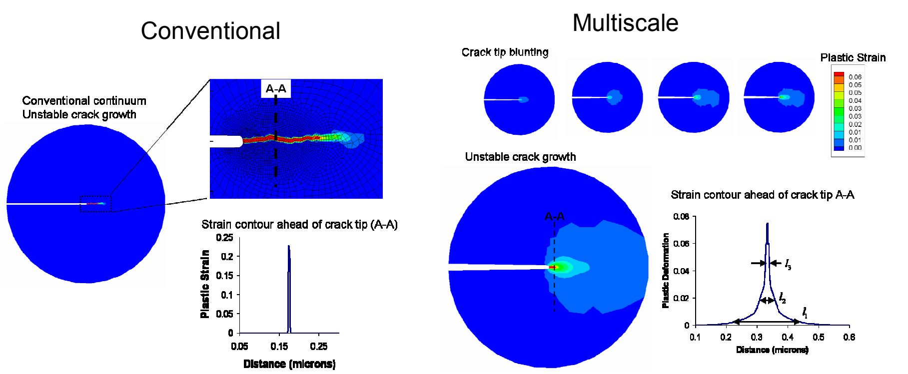

Multiscale Fracture Toughness (WC-Co)

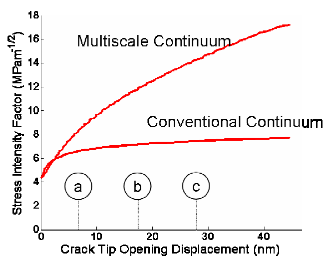

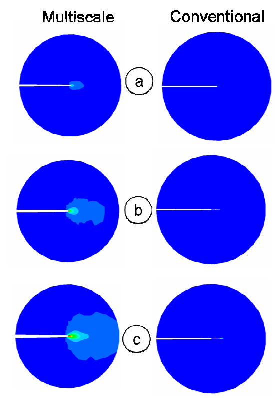

Blunting predicted by Multiscale model ; Toughness approaches experimental values

Multiscale Fracture Toughness (WC-Co)

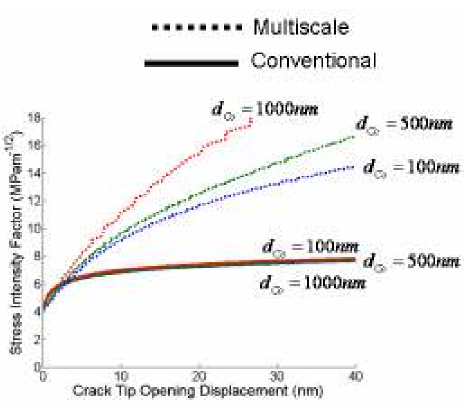

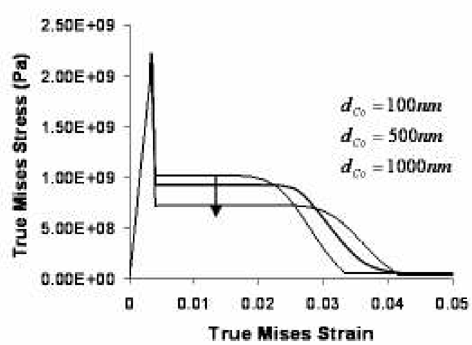

- Conventional model predicts decreasing toughness with grain size
- Multiscale model predicts increasing toughness
    - extra crack blunting as physical length scale increases

Multiresolution Constitutive Relations, Materials Instability Points, and Equations of States

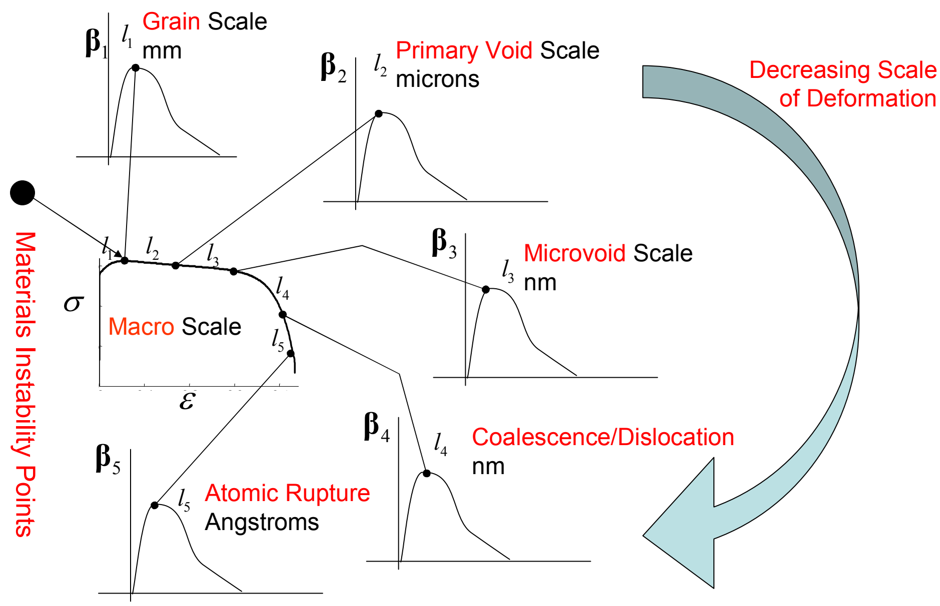

Reduction of the # DOF

Problem: # degrees of freedom increases with scale

E.g. Four scale problem has 14 d.o.f. per node

Microstresses are successively dominant

Solution: Use a single microstress, which is active at different scales

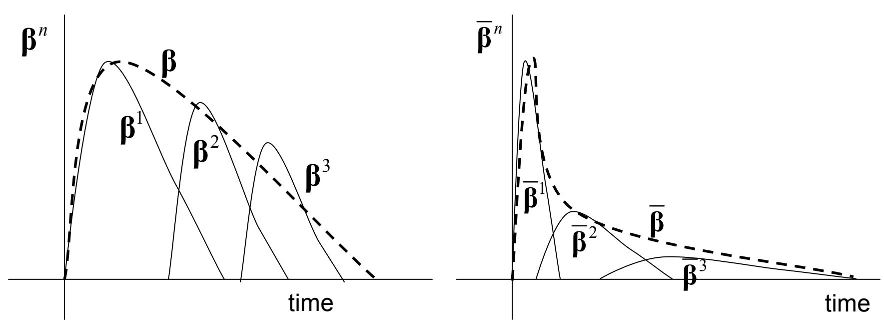

$$\nabla\cdot\left(\boldsymbol{\sigma}-\boldsymbol{\beta}^{msT}\right)+\mathbf{b}=0 \quad \text{in} \quad \Omega$$
$$\nabla\cdot\bar{\boldsymbol{\beta}}^{ms}-\boldsymbol{\beta}^{ms}+\mathbf{B}=0 \quad \text{in} \quad \Omega$$
$$\mathbf{t}=\mathbf{N}\cdot\left(\boldsymbol{\sigma}-\boldsymbol{\beta}^{msT}\right) \quad \text{on} \quad S$$
$$\mathbf{R}=\mathbf{rN}=\mathbf{N}\cdot\bar{\boldsymbol{\beta}}^{ms}:(\mathbf{NN}) \quad \text{on} \quad S$$
$$\bar{\beta}^{ms}=\left(l^{ms}\right)^{2}E\nabla\boldsymbol{\varepsilon}^{ms}$$

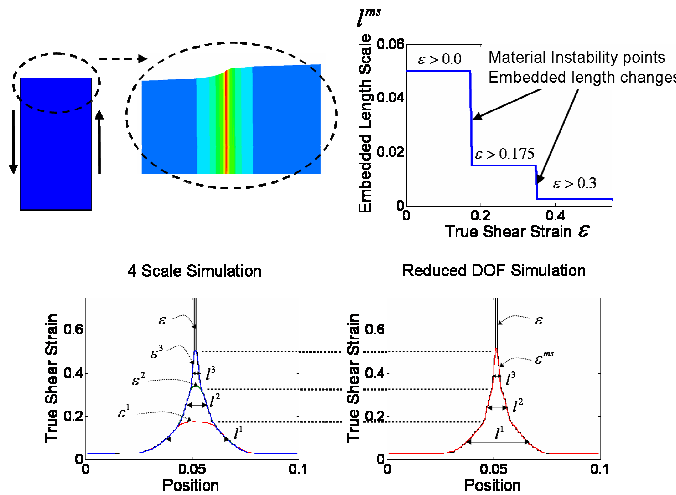

- Multiscale microstress acts at each scale successively
- Embedded length scale changes at the instability points
- Replicates the multiscale analysis with fewer degrees of freedom
- Relatively inexpensive compared to the multiscale continuum and DNS
- Behaves as a variable length scale gradient theory

Extension to Multiscale Multiphysics

- Thermal, electrical and mass diffusion equations are similar to the mechanical equation

- Length scales can be embedded in each to describe local effects

Governing Equations

$$\left(\mathbf{q}-\sum_{n=1}^{N}\mathbf{p}^{n}\right)\cdot\bar{\nabla}+Q=\mu\dot{\theta}$$
$$\bar{\mathbf{p}}^{n}\cdot\bar{\nabla}-\mathbf{p}^{n}+\mathbf{R}^{n}=\dot{\theta}^{n}\bar{\nabla}\cdot\mathbf{I}^{n}$$

Boundary conditions

$$\left(\mathbf{q}-\sum_{n=1}^{N}\mathbf{p}^{n}\right)\cdot\mathbf{n}=\tilde{q}$$
$$\bar{\mathbf{p}}^{n}\cdot\bar{\nabla}=\mathbf{r}^{n}$$

Constitutive Relationships

$$\mathbf{q}=-\mathbf{k}\cdot\bar{\nabla}\theta$$
$$\mathbf{p}^{n}=-\mathbf{k}\left(\bar{\nabla}\theta^{n}-\bar{\nabla}\theta\right)$$
$$\bar{\mathbf{p}}^{n}=-\mathbf{k}l^{2}\left(\bar{\nabla}^{2}\theta^{n}\right)$$

General Problem → / **Specific Problem** ↓	**Constant** μ	**Flux** $\mathbf{q}$	**Potential** θ	**Conductivity** $\mathbf{k}$	**Internal Source** Q	**Boundary Flux** $\tilde{q}$
Thermal	Density × Specific Heat $\mu_t=\rho c(\theta_t)$	Heat flux $\mathbf{q}_t$	Temperature θ_t	Thermal Conductivity $\mathbf{k}_t(\theta_t)$	Internal Heat Generation Q_t	Boundary Heat Flux $\tilde{q}_t$
Electrical	(Steady state) $\mu_e=0$	Electrical Current flow $\mathbf{q}_e$	Voltage θ_e	Electrical Conductivity $\mathbf{k}_e(\theta_t)$	Internal Current Source Q_e	Externally Applied Boundary Current $\tilde{q}_e$
Mass Diffusion	$\mu_m=1$	Flux of concentration of diffusing phase $\mathbf{q}_m$	Concentration θ_m	Diffusivity $\mathbf{k}_m(\theta_t)$	Internal Source Flow Q_m	Boundary Mass Flux $\tilde{q}_m$

Multiresolution, Multiphysics

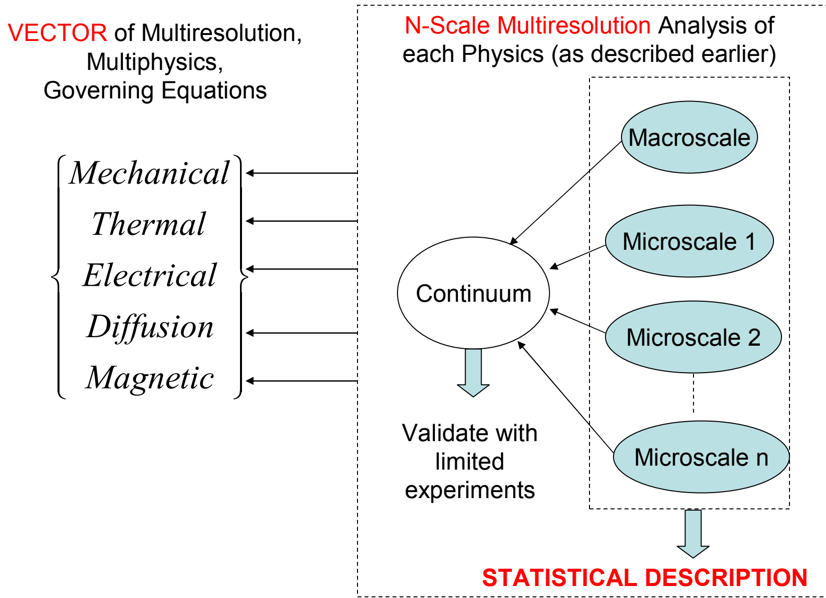

Fuel Cell

- Fuel cell is an electrochemical device which converts chemical energy to electrical energy

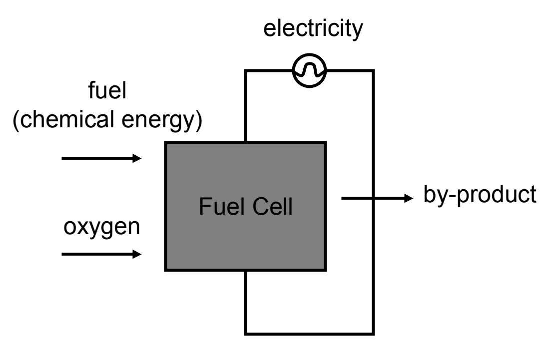

Fuel cells will work as long as fuel and oxygen are supplied.

Types of Fuel Cells

- **Polymer electrolyte membrane fuel cell (PEMFC)**
  - hydrogen or methanol
  - proton conducting polymer membrane electrolyte, platinum coated porous carbon electrode, 80-110^{o}C
  - high power density, low operating temperature
  - expensive components, contamination
  - automotive
- **Solid oxide fuel cell (SOFC)**
  - hydrogen
  - solid metal oxide electrolyte, porous conducting cermet/oxide electrode, 600-1000^{o}C
  - waste heat, high power density
  - high temperature issues, expensive, sealing
  - stationary power generator

Carrette et al, Chemphyschem, 2000
http://www.nfcrc.uci.edu/fcresources/FCexplained/index.htm
O'Hayre R, Cha SW, Colella W, Prinz FB, Fuel Cell Fundamentals, John Wiley & Sons, New York, 2006

Types of Fuel Cells

- **Phosphoric acid fuel cell**
  - hydrogen
  - liquid H_3PO_4 electrolyte, platinum coated graphite electrode, 160-200^{o}C
  - mature technology, low cost
  - susceptible to catalyst contamination, electrolyte evaporation
  - commercial power generator for building
- **Alkaline fuel cell**
  - hydrogen
  - aqueous KOH electrolyte, platinum coated porous carbon or nickel electrode, 60-90^{o}C
  - low cost
  - pure H_2 and O_2, remove water, resupply electrolyte
  - aerospace
- **Molten carbonate fuel cell**
  - hydrogen, methane, alcohol
  - molten alkali carbonate electrolyte, porous nickel electrode, 600-800^{o}C
  - fuel flexibility, high quality waste heat
  - CO_2 recycling, degradation, expensive materials

Charges and Ions

- **Electric charge** is a fundamental conserved property of some subatomic particles, which determines their electromagnetic interaction.

- An **ion** is an atom or group of atoms that normally are electrically neutral and achieve their status as an ion by loss or addition of one or more electrons

http://en.wikipedia.org/wiki/Ion
http://en.wikipedia.org/wiki/Electric_charge

How Do Fuel Cells Work

Electrons are transported through external circuit (Interconnects) delivering electric power.

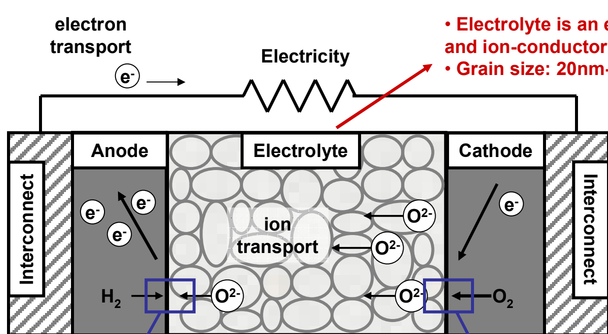

• Electrolyte is an electron-insulator and ion-conductor.
• Grain size: 20nm-few μm

At the anode, hydrogen is oxidized into water and electrons.

$$H_2 + O^{2-} \rightarrow H_2O + 2e^-$$

Oxygen ions are transported through an ion conducting electrolyte

At the cathode, oxygen is reduced to oxygen ions.

$$\frac{1}{2}O_2 + 2e^- \rightarrow O^{2-}$$

electron transport via interconnect

generate **electrons** → consume **electrons**

consume **oxygen ions** ← generate **oxygen ions**

oxygen ion tranport via electrolyte

Solid Oxide Fuel Cell (SOFC)

- SOFCs employ a oxide membrane as an electrolyte, which is doped to have ionic conductivity.
- To achieve enough ion conductivity, operating temperature needs to be high (600-1000^{o}C).
- Typical fuel cell design forms a “stack” of individual cells to produce enough voltage.

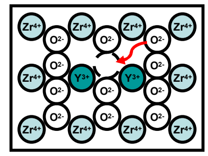

YSZ

Planar SOFC stack

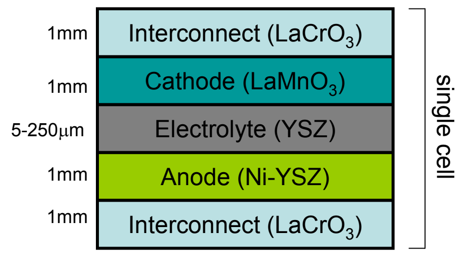

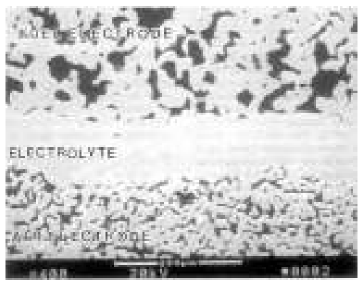

YSZ: yttrium stabilized zirconia
$LaMnO_3$: lanthanum manganite
$LaCrO_3$: lanthanum chromite
Ni: nickel

Singhal SC, Solid State Ionics, 2000

SOFC Components

- Common requirements: chemical and material stability at high temperatures, no reaction with other components, minimum thermal expansion mismatch
- Electrolyte (**Electrolyte is an electron-insulator and ion-conductor)**
  - Role: path for oxygen ions from cathode to anode
  - Requirements: high conductivity for ions, low conductivity for electrons, gas-tightness
  - Materials: yttria stabilized zirconia, gadolinia doped ceria
- Anode
  - Role: reaction site for oxidation reaction to yield electrons (electricity)
  - Requirements : porosity(30-40%) for fuel flow, high conductivity for electrons
  - Materials: nickel-yttria stabilized zirconia composite, nickel-ceria composite
- Cathode
  - Role: reaction site for reduction reaction to yield ions
  - Requirements: porosity(30-40%) for air flow, high conductivity for electrons
  - Material: strontium-doped lanthanum manganite
- Interconnect
  - Role: providing electrical contact between cells, distributing fuel to anode and air to cathode
  - Requirements: electron conductivity, impermeability
  - Material: lanthanum chromite

Badwal, Ceramic International, 1996
Ormerod, Chemical Soceity Reviews, 2002

SOFC Performance and Operating Temperature

- Current operating temperature is 800-1000°C.
- Lower operating temperature can reduce fuel cell degradation and allow cheaper materials for interconnects and seals.
- However, efficiency drops as temperature decreases.
- In order to decrease operating temperature while maintaining efficiency, it is necessary to develop electrolyte materials with enhanced oxygen conductivity.
- Nano-scale oxides with high surface area will offer a great opportunity to increase oxygen conductivity and lower operating temperature.

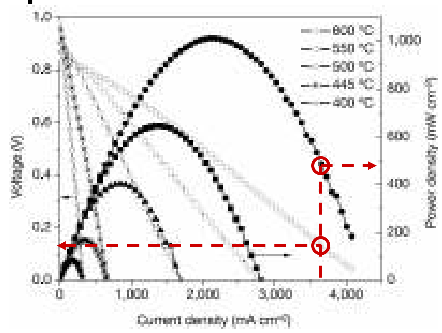

Voltage and power density versus current density*

- For a given current density, the voltage is measured. Or for a given voltage, the current density is measured.
- Power density is the product of voltage and current density.
- Efficiency is proportional to the voltage.
- Voltage drops as current increases because of
1. Activation loss due to electrochemical reaction
2. Ohmic loss due to ionic and electronic conduction
3. Concentration loss due to mass transport of hydrogen and oxygen

*Shao and Haile, Nature, 2004

Our Focus: Reliability Issues

- Long term performance and reliability have not been demonstrated by detailed modeling.
  - Endurance and longevity
  - Thermal cycling capability:
    During thermal cycle, the difference between coefficients of thermal expansion of electrolyte and electrodes causes residual stress, which may lead to fracture.
  - Durability in installed environment (seismic, transportation, space)

Thermomechanical Failures in Electrolytes

- Factors affecting residual stress
  - coefficient of thermal expansion
  - processing temperature and operation temperature
  - elastic constant (affected by dopant content, oxygen partial pressure)
  - thickness
- Difference in thermal expansion coefficients between the planar SOFC stack layers can be 5-25%*.
- Residual stresses can be 10-200MPa*, which may exceed critical stress of failure.

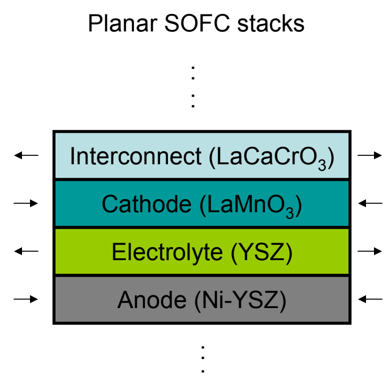

*Montross et al, British Ceramic Transactions, 2002

Solid Oxide Fuel Cell: Electrolyte

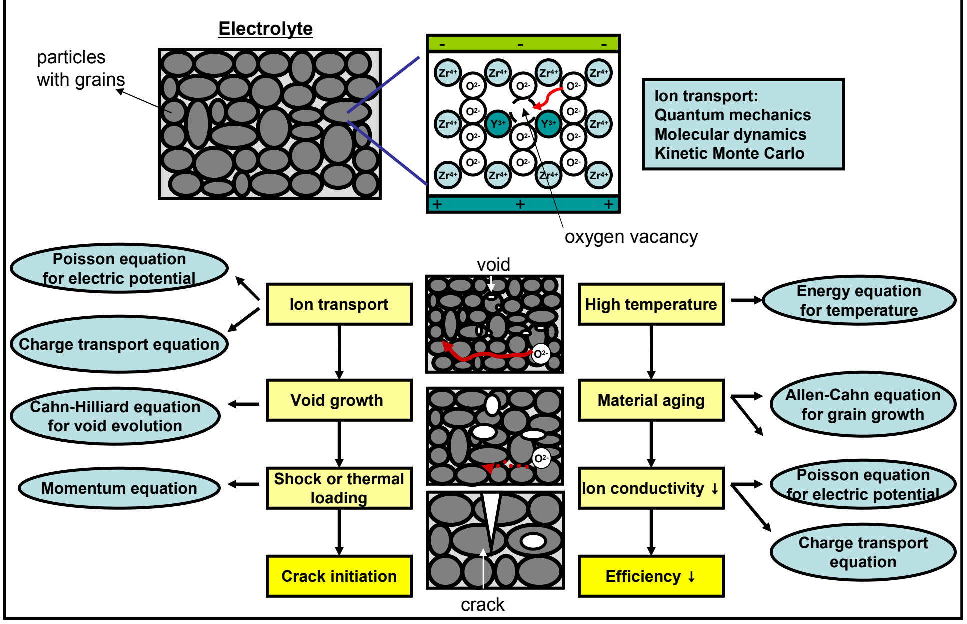

Solid Oxide Fuel Cell: Anode

Ni-YSZ cermet

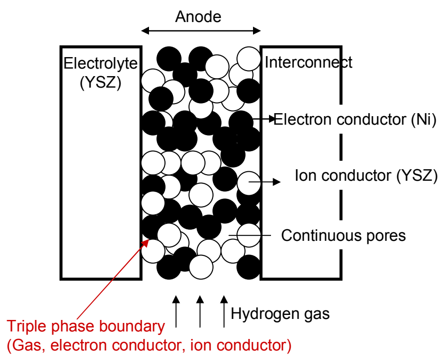

Role

Ni: transporting electrons, catalyst

Yttria stabilized zirconia (YSZ): matching thermal expansion, inhibiting Ni coarsening, transporting ions

Pore: diffusion path for hydrogen gas

Triple phase boundary: electrochemical reaction site

Microstructure parameters

volume fraction
porosity
size distribution
size ratio

Desired material properties

Large electrical conductivity
Large gas diffusion coefficient
Low anode overpotential

Degradation mechanisms

Ni coarsening → discontinuity, decrease of reaction site
Ni creep → deformation

Equations

Momentum equation
Ohm's law
Heat transfer equation
Cahn-Hilliard equation
Butler-Volmer equation
Diffusion equation

Solid Oxide Fuel Cell: Cathode

Doped lanthanum manganite

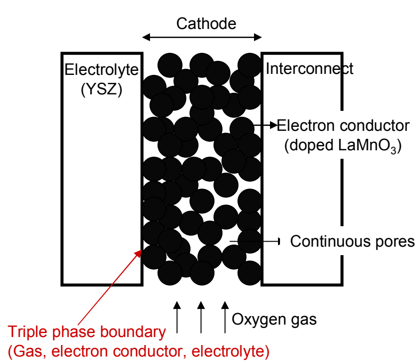

Role

Doped $LaMnO_3$: transporting electrons

Pore: diffusion path for oxygen gas

Triple phase boundary: electrochemical reaction site

Microstructure parameters

volume fraction
porosity
size distribution
size ratio
dopant level

Desired material properties

Large electrical conductivity
Large gas diffusion coefficient
Low cathode overpotential

Equations to solve

Momentum equation
Ohm's law
Heat transfer equation
Butler-Volmer equation
Diffusion equation

Microstructure of Ni-YSZ cermet (anode material) is modeled by phase-field model.

pure Ni conductivity 1.431E7 S/m

YSZ conductivity 0.1 S/m

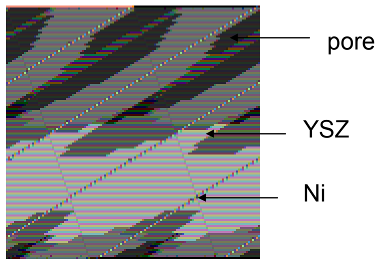

Ni: 56% YSZ: 17%

conductivity 1.123E7 S/m

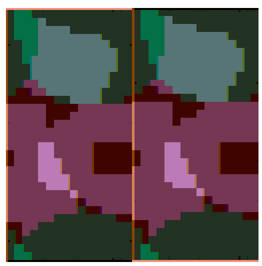

Ni: 30% YSZ: 43%

conductivity 16 S/m

Higher nickel content gives better conductivity.

The cell performance is calculated using the anode properties obtained previously.

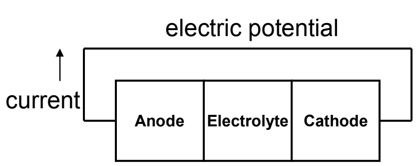

anode thickness: 100mm
electrolyte thickness: 10mm
electrolyte conductivity 0.1 S.cm

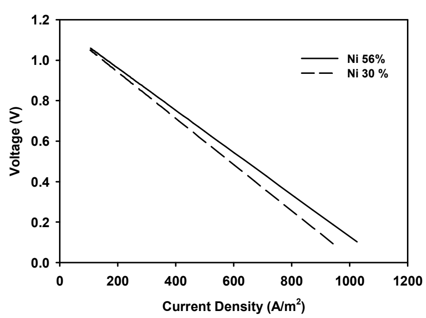

Higher nickel content gives better performance.

The effects of other parameters (particle size, reaction site) will be studied.

Solid Oxide Electrolyte Design: Zirconia/Alumina Composite

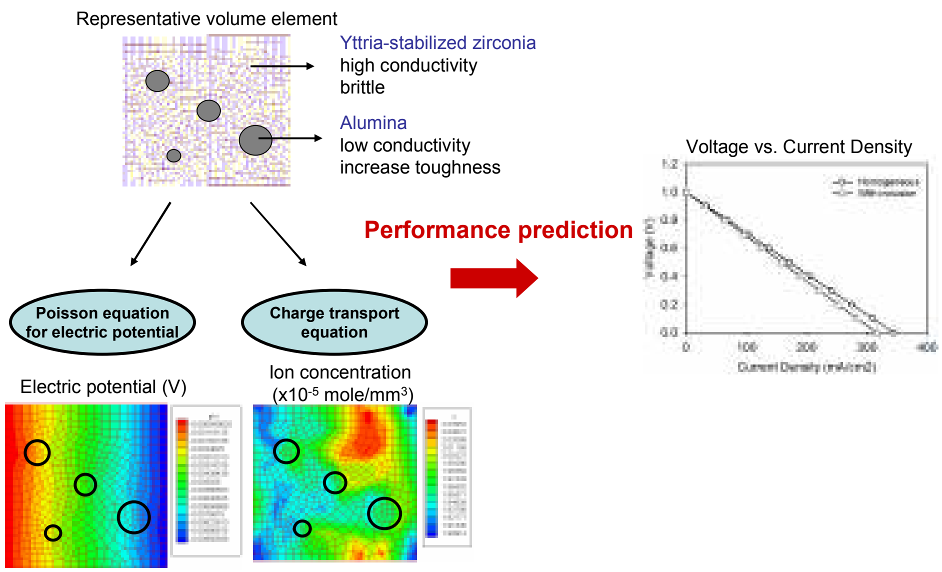

Motivations for Thermoelectric Material

- The US and global economic growth is shadowed by shrinking energy resource
- Existing industrial processes are inefficient and produce large amount of waste heat and harmful emissions (an example below)

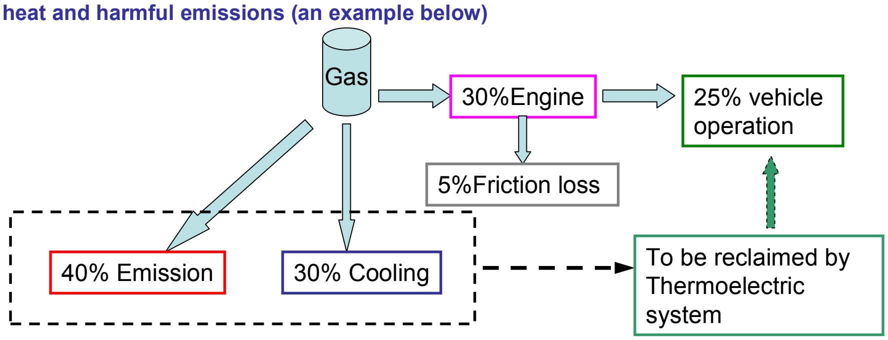

- Advantages of Thermoelectric material
  - Directly convert thermal energy to electricity
  - No emission of harmful waste
  - Can be used for thermal management of small scale circuits
  - Requires little supervision and can be used as steady energy supplies

Work with Prof. Dong Qian at the University of Cincinnati

Thermoelectric Material: Basic Mechanisms

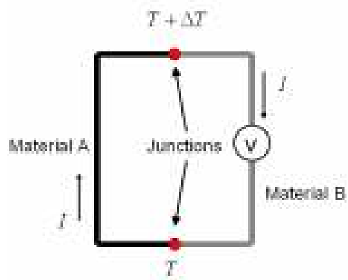

•Power Generation: Seebeck effect (1821)
If different temperatures are maintained at
The two junctions, electric current will develop.

• Electric Cooling: Peltier effect (1834)
If electric current passes through the same thermocouple, heat will be transferred from one junction to the other .

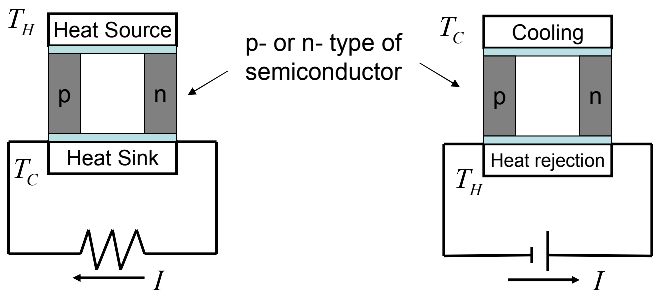

Typical Thermoelectric Module (L) power generation (R) Electric Cooling

Work with Prof. Dong Qian at the University of Cincinnati

Thermoelectric Material: Power conversion efficiency

•The potential of thermoelectric application is measured by power conversion efficiency (in the case of Seebeck effect)

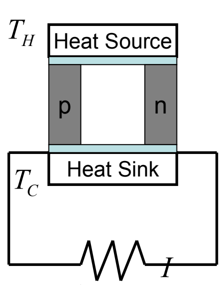

$$\phi = \frac{\text{Electric Energy Generated}}{\text{Heat Energy Absorbed}}$$

•Maximum Power conversion efficiency can be achieved is

Canot Efficiency: thermodynamic limit

$$\phi_{\max} = \boxed{\frac{T_H - T_C}{T_H}} \left(1 - \frac{1 + T_C / T_H}{\sqrt{1+ZT} + T_C / T_H} \right)$$

•Power conversion efficiency depends on the product of figure-of-merit *Z* with average temperature *T*

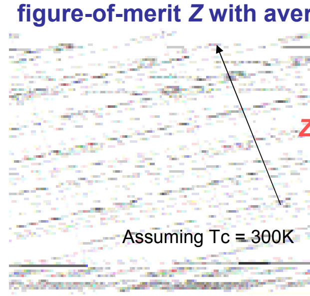

***ZT* shall be as high as possible!**

Work with Prof. Dong Qian at the University of Cincinnati

Thermoelectric Material: How to control *ZT*?

•*ZT* is also referred to as the dimensionless figure-of-merit, determined by

Seebeck coefficient   electrical conductivity   temperature

$$ZT = \frac{\alpha^2 \sigma T}{\kappa}$$

thermal conductivity

•Since temperature is controlled by application, current thermoelectric material research mainly focuses on

- **Reducing thermal conductivity**
- **Improving Seebeck coefficient and electric conductivity**
- **Two different research directions:**
  - ❑ Bulk material systems
  - ❑ Low-dimensional material systems

Work with Prof. Dong Qian at the University of Cincinnati

Seebeck Effect

- An electric current flows in a closed circuit made up of two dissimilar metals, if the junctions of the metals are maintained at two different temperatures (Seebeck, 1821).

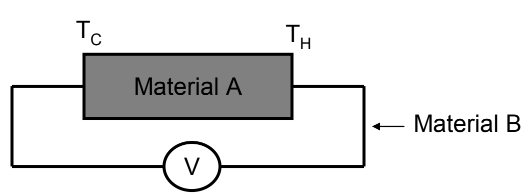

Seebeck coefficient or Thermopower $\alpha = \frac{dV}{dT}$

V: electric potential
T: temperature

Thermoelectric Material: Developments in Bulk Material System

•The basic concept is to create strong phonon scattering by introducing guest atoms (rattlers) into partially-filled structural sites

Phonon relaxation time

Thermal conductivity $\kappa \propto \tau$

Phonon scattering increase values of $\frac{1}{\tau}$

→ Reduced thermal conductivity

• Existing material systems include skutterudites, clathrates, complex chalcogenides, half-Heusler alloys, oxide materials and many others

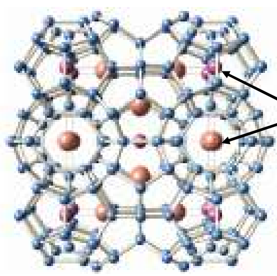

Guest atoms

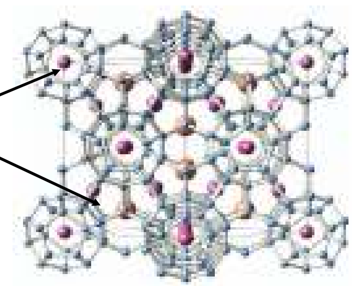

Crystal structures of Clathrate (Type I)
Nolas et al, *MRS bull.*, 2006

Crystal structures of Clathrate (Type II)
Nolas et al, *MRS bull.*, 2006

Work with Prof. Dong Qian at the University of Cincinnati

Thermoelectric Material: Developments in Bulk Material System

Current developments seem to face a bottleneck of *ZT* at ~ 1.

•State-of-the-art thermoelectric material such as SiGe-based alloys for space applications achieve power conversion efficiency of ~8%.

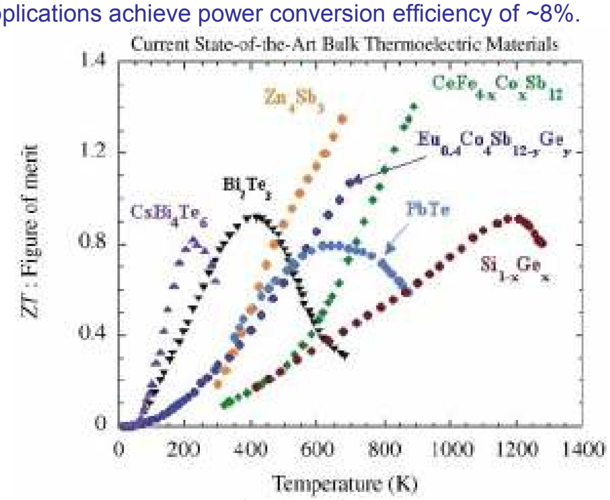

Tritt in *Encyclopedia of Materials: Science and Technology*, 2002.

Work with Prof. Dong Qian at the University of Cincinnati

Thermoelectric Material: Developments in low-dimensional Material System

•Development centers on the concept of "superlattices" thin film systems

•Superlattices are created by stacking periodically alternating thin layers of different materials

- ➢The electronic performance may be improved due to the reduced length scale (quantum confinement effect)
- ➢Alternating layers create interface for phonon scattering

• Developed material systems include Bi_2Te_3/Sb_2Te_3 and Bi_2Te_3/Bi_2Se_3, and PbSeTe/PbTe quantum dot superlattices. *ZT* value approaches to 4.

TEM image of alternating layers of Bi_2Te_3/Sb_2Te_3 superlattice

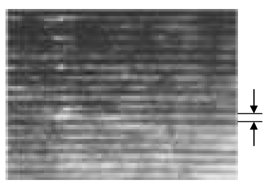

Touzelbaev, *JAP*, 2001

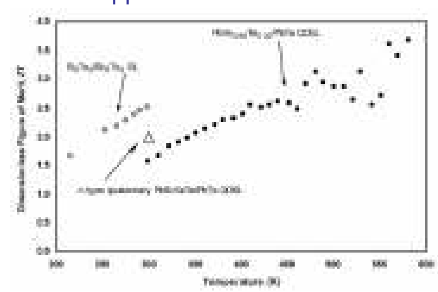

Bottner et al, *MRS bull.*, 2006

Work with Prof. Dong Qian at the University of Cincinnati

Thermoelectric Material: Current Trends

•Integrating low-dimensional micro/nano material into bulk systems.

- ➢The advance in synthesis reveals a number of nanomateial systems with excellent electronic conductivities

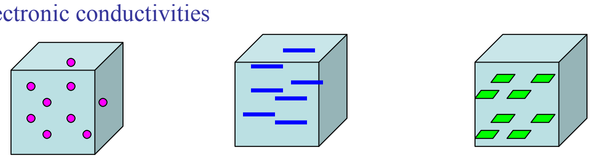

nanoparticles | Nanowires/tubes | Nanosheets

- ➢The large surface-to-volume ratio at small scale may leads to much enhanced phonon scattering and reflection, which is the key to reduced thermal conductivity
- ➢The excellent physical properties of nanomaterials may also enhance other properties of the bulk material system (strength and stiffness, fracture toughness, …)

• Significant challenges remain in the analytical and numerical evaluation of the thermoelectric performance.

- ➢ Multiple length scales and mechanisms
- ➢ Proper treatment of the interface
- ➢ Coupling among electronic, thermal and mechanical fields

Work with Prof. Dong Qian at the University of Cincinnati

Thermoelectric Material Design: Bismuth Telluride Nanotube Composite

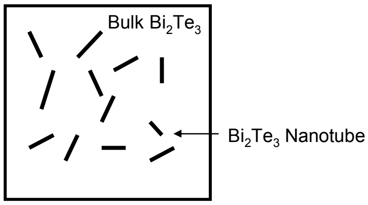

Bismuth telluride nanotubes

Zhao et al, Appl Phys Letters, 2005

Desired properties
High electrical conductivity
Low thermal conductivity

Nanotube: phonon scattering center
→ decrease thermal conductivity

Design parameters
Volume fraction
Nanotube size

Equations to solve
Phonon Boltzmann equation

Thermoelectric Materials: Multiphysics Design

$$ZT = \frac{\alpha^2 \sigma T}{\kappa}$$

α: Seebeck coefficient
σ: electrical conductivity
κ: thermal conductivity
T: temperature

Good thermoelectric material should have a high ZT value.

→ High Seebeck coefficient → $\alpha \approx \frac{E_g}{k_B T}$

E_g: bandgap
k_B: Boltzmann constant

$$\alpha \approx \frac{\alpha_n \sigma_n + \alpha_p \sigma_p}{\sigma_n + \sigma_p}$$

p: hole
n: electron

large enough bandgap to reduce minority carrier contribution

→ High electric conductivity → reduce bandgap

$$\sigma = \sigma_0 \exp(-E_g / k_B T)$$

increase mobility of carriers

→ Low thermal conductivity → $\kappa_E = \sigma L T$

L: Lorenz number

$$\kappa = \kappa_E + \kappa_L$$

$$\kappa_L \approx \frac{1}{3} v_s C L_{ph}$$

v_s: speed of sound
C: heat capacity
L_{ph}: mean free path of phonons

κ_E: thermal conductivity due to electrons
κ_L: thermal conductivity due to lattice vibration

reduce mean free path of phonons

Work with Prof. Dong Qian at the University of Cincinnati

Solving Band Gap for Periodical Solids: Bloch's Theorem

Real Space **Reciprocal Space**

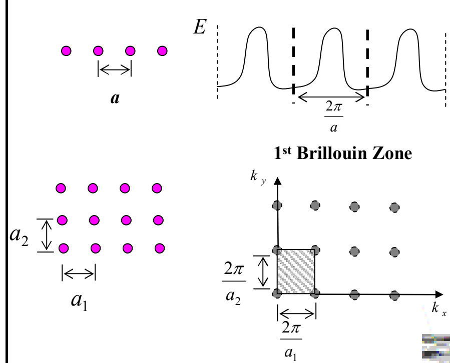

Bloch's Theorem: The eigenfunctions of the wave equation for a periodic potential are the product of a plane wave $e^{ik\cdot r}$ times a function $u_k(r)$ that has the periodicity of the lattice.

$$H|\psi(\mathbf{r})\rangle = \left[-\frac{\hbar}{2m}\nabla^2 + V(\mathbf{r})\right]|\psi\rangle = E|\psi\rangle$$

$$\Leftarrow V(\mathbf{r}) = V(\mathbf{r}+\mathbf{r}_n)$$

Periodicity

$$|\psi_k(\mathbf{r})\rangle = u_k e^{-ik\cdot r}$$

The electronic band structure can be obtained by Sampling *k* within the 1st Brillouin zone

Shortcomings of the approach
1) First-principle methods are expensive
2) Coupling with Mechanical deformation typically not accounted for.

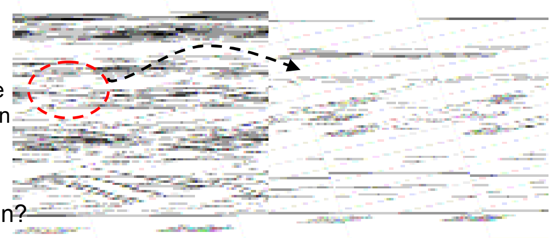

Can we develop a continuum version?

Obtaining Band Gap using a multiscale approach:
Coupling Continuum model with quantum-mechanical method

- A **Three-way Coupling Approach (Qian and Liu, *CMAME (submitted), 2007)***

QM **MD** **FEM/Meshfree**

$$\boxed{H|\psi\rangle = E|\psi\rangle} \Leftrightarrow \boxed{m_\alpha \ddot{\mathbf{u}}_\alpha = -\frac{\partial E}{\partial \mathbf{r}_\alpha}} \Leftrightarrow \boxed{\mathbf{N}^T \mathbf{f}_\alpha(\mathbf{u}) = \mathbf{N}^T m_\alpha \ddot{\mathbf{u}}_\alpha}$$

1. Quantum mechanical method solves the electronic wave functions $|\psi\rangle$ and the Energy states E. The spatial derivative of E gives the inter-atomic interactions

2. The continuum (virtual atom cluster) model solves the FEM equation based on the inter-atomic interactions.Provide the updated atomic position.

3. Based on the new atomic position, the Schrodinger equation is being solved for The next step.

Example: Multiscale Study of Band Gap in Carbon Nanotubes

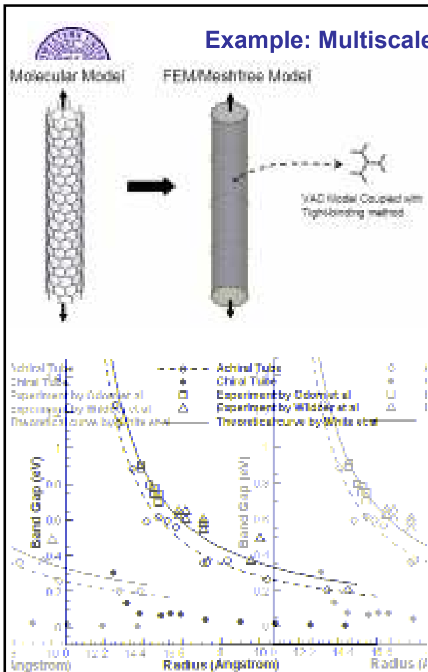

- Band gap Eg decreases as radius increases
- Band gap trends for (n,m) tube if *mod* (n-m) ≠ 3 (achiral)

This calculation	$E_g \propto r^{-1.056}$
Theoretical estimate (no relaxation and rehybridization effect) (White, et al. *Carbon*, 1993)	$E_g \propto r^{-1}$

- Band gap trends for (n,m) tube if *mod* (n-m) = 3 (chiral)
  - Moderate band gap is observed when radius is less than 4 Å
  - It decreases rapidly between 2 and 4 Å.
  - After the radius is greater than 6 Å, narrow band gaps

Work with Prof. Dong Qian at the University of Cincinnati

Example: Band Gap in Carbon Nanotubes due to Tension

- The band gap in (10,10) tube is not sensitive to the applied tension and it remains metallic at all the imposed strains
- The transition from metallic to semi-concdutor or vise versa is observed for a number of tubes (S-M or M-S)
- The band gap changes in most of the tubes show a linear trend as a function of the applied strain
- Comparison with other results (below)

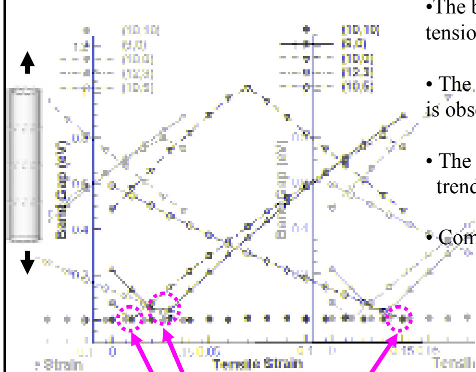

S-M or M-S transtion

	This calculation	Others*
Band gap in (9,0) tubes at 0% strain	0.22 eV	0.2 eV
Band gap in (9,0) tubes at 15% strain	0.89 eV	0.86 eV
S-M transition strain in (9,0) tubes	2%-3%	2%-3%

*Yang et al, CMES, 2002
Liu et al, JMPS, 2004

Virtual Multiscale Life Cycle Nano and Microstructural Materials Design

Device Scale Continuum computes
• Stress (Strain), Temperature
• Electric potential, Concentration
→
Requires
• Average Grain size, Porosity,

Mesoscale Sample Region computes
• Grain Boundary Motion
• Void Evolution
→
Requires
• Diffusion coefficients
• Nucleation of voids
• Free energy

KMC & MD Sample Region computes
• Vacancy diffusion i.e. void nucleation
→
Requires
• Initial vacancy distribution
• Atomic behavior (potential)

QM computes
• Interatomic Potential for MD and KMC

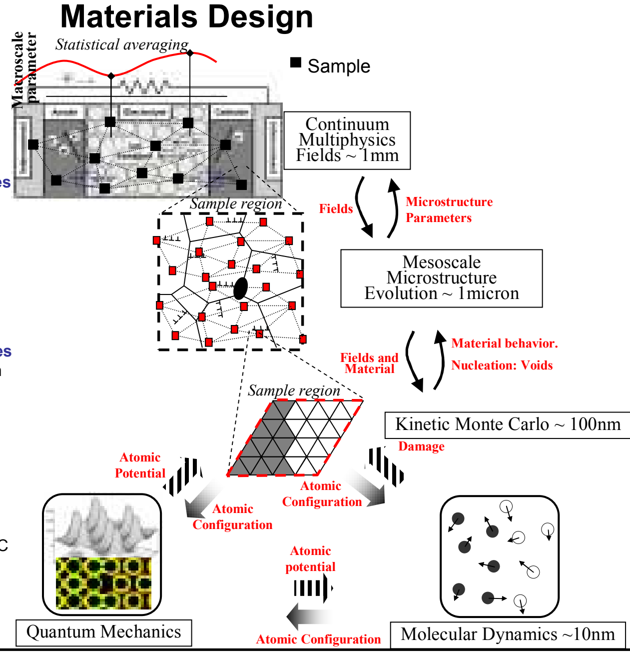

Fracture Behavior under Shock Load (milliseconds)

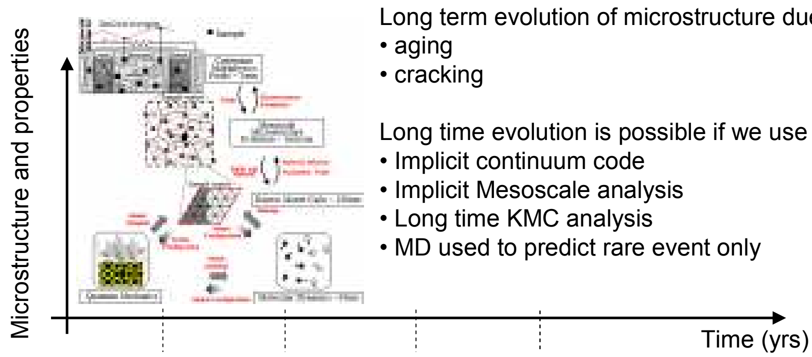

Long term evolution of microstructure due to
• aging
• cracking

Long time evolution is possible if we use
• Implicit continuum code
• Implicit Mesoscale analysis
• Long time KMC analysis
• MD used to predict rare event only

• Retrieve microstructure and properties at various intervals

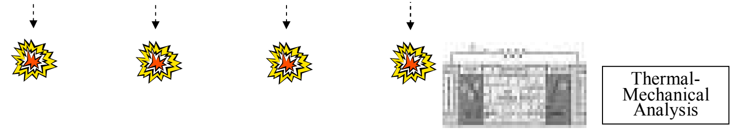

• Perform shock loaded Thermal-mechanical Dynamic-Explicit Fracture Simulation
• XFEM, crack tip MD, Concurrent Discrete Microstructure -Continuum theory, Multiscale Continuum theory

Governing Equations

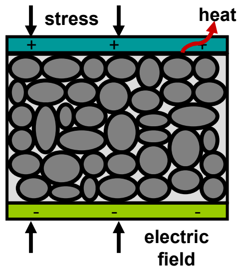

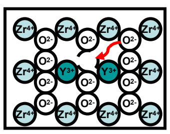

charge transport

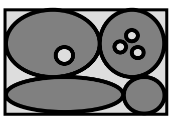
grain growth
void migration

Momentum equation	$\nabla \cdot \boldsymbol{\sigma} + \mathbf{b} = \rho \dot{\mathbf{v}}$	velocity, stress
Energy equation	$\rho C_p \frac{\partial T}{\partial t} = \nabla \cdot (\kappa \nabla T)$	temperature
Poisson equation	$\nabla \cdot (\varepsilon \nabla \Phi) = -\sum_i q_i e c_i$	electric potential
Charge transport equation	$\frac{\partial c_i}{\partial t} = \nabla \cdot D \left(\nabla c_i + \frac{q_i e c_i}{kT} \nabla \Phi \right)$	ion concentration
Allen-Cahn equation for grain coarsening	$\frac{\partial \eta_i}{\partial t} = -L \frac{\delta F}{\delta \eta_i}$	grain orientation
Cahn-Hilliard equation for void migration	$\frac{\partial \rho}{\partial t} = \nabla \cdot \left(M \left(\nabla \frac{\delta F}{\delta \rho} - \theta \nabla \Phi \right) \right)$	density

Variables and Parameters

$$\nabla \cdot \boldsymbol{\sigma} + \mathbf{b} = \rho \dot{\mathbf{v}}$$

$$\rho C_p \frac{\partial T}{\partial t} = \nabla \cdot (\kappa \nabla T)$$

$$\frac{\partial c_i}{\partial t} = \nabla \cdot D \left(\nabla c_i + \frac{q_i e c_i}{kT} \nabla \Phi \right)$$

$$\nabla \cdot (\varepsilon \nabla \Phi) = -\sum_i q_i e c_i$$

$$\frac{\partial \eta_i}{\partial t} = -L \frac{\delta F}{\delta \eta_i}$$

$$\frac{\partial \rho}{\partial t} = \nabla \cdot \left(M \left(\nabla \frac{\delta F}{\delta \rho} - \theta \nabla \Phi \right) \right)$$

Symbol	Name	Method to obtain parameter
$\boldsymbol{\sigma}$	stress	
$\mathbf{b}$	body force per unit volume	
ρ	density	
$\mathbf{v}$	velocity	
C_p	specific heat	
T	temperature	
t	time	
κ	thermal conductivity	transport theory; MD
S	heat generation rate	
Φ	electric potential	
e	charge of an electron	
c_i	concentration of species i	
q	charge number	
ε	permittivity	
D	diffusivity	first principles calculation + transport theory
η_i	field parameter for grain orientation	
L	kinetic coefficient	experiment
M	kinetic coefficient	experiment
Θ	effective charge	
F	Free energy	

DoE Advanced Simulations Computing: Diffusional Creep

Boeing Design **Honeywell Design**

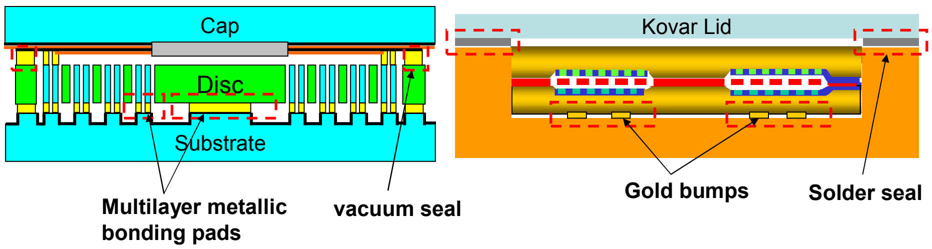

Ex: Grain Boundary Diffusional Creep (JS Chen, UCLA)

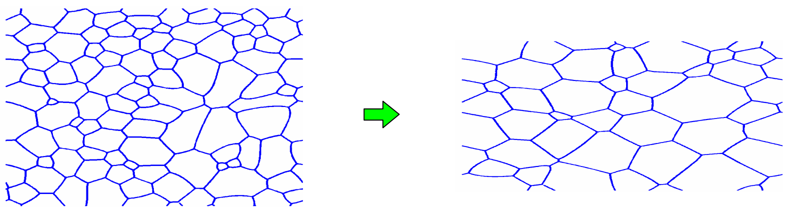

Summary

(i) Micromechanical simulations allow us to:

- Investigate failure mechanisms in existing and novel materials
- Develop predictive micromechanical based constitutive relationships

(ii) Extension of continuum theory to multiple scales of inhomogeneous deformation

- Predict process zone behavior in terms of the microstructure
- Macroscale response with a microscale resolution where necessary

Currently….

- Introduction of a statistical dependence in the constitutive relationships
- Extension to thermal-mechanical-mass diffusive continuum systems
- Computational science-based mathematical framework
- Verification and validation through limited experiments
- LIFE-CYCLED NOVEL MATERIALS DESIGN through the use of Petaflop Computing.

References

Review on fuel cells

1. Carrette L, Friedrich KA, Stimming U, Chemphyschem 1, 162 (2000)
2. Minh NQ, J Am Ceram Soc 76, 563 (1993)
3. Badwal SPS, Foger K, Ceramics International 22, 257 (1996)
4. Brandon NP, Skinner S, Steele BCH, Annu Rev Mater Res 33, 183 (2003)
5. Ormerod RM, Chem Soc Rev 32, 17 (2003)
6. Ralph JM, Schoeler AC, Krumpelt M, J Mater Sci 36, 1161 (2001)
7. O'Hayre R, Cha SW, Colella W, Prinz FB, Fuel Cell Fundamentals, John Wiley & Sons, New York, 2006

SOFC electrolyte

1. Goodenough JB, Annu Rev Mater Res 33, 91 (2003)
2. Badwal SPS, Ciacchi FT, Ionics 6, 1 (2000)

SOFC electrolyte grain size effect

1. Tschope A, Ying JY, Nanostruc Mater 4, 617 (1994)
2. Chiang YM, Lavik E , Kosacki, Tuller HL, Ying JY, J Electroceramics 1, 7 (1997)
3. Suzuki T, Kosacki I, Anderson HU, J Am Ceram Soc 85, 1492 (2002)
4. Kosacki I, Petrovsky V, Anderson HU, J Am Ceram Soc 85, 2646 (2002)
5. Suzuki T, Kosacki I, Anderson HU, Solid State Ionics 151, 111 (2002)
6. Kosacki, Anderson HU, Mizutani Y, Ukai K, Solid State Ionics 152-153, 431 (2002)
7. Kosacki I, Suzuki T, Petrovsky V, Anderson HU, Solid State Ionics 136/137, 1225 (2002)
8. Boaro M, Torvarelli A, Hwang JH, Mason TO, Solid State Ionics 147, 85 (2002)
9. Maier J, "Nanoionics and soft materials science" in Nanocrystalline Metals and Oxides: Selected Properties and Applications, P. Knauth and J. Schoonman, Eds., Kluwer Academic Publishers, Norwell, MA (2002) p. 81

References (cont'd)

SOFC YSZ/Alumina composite electrolyte

1. Navarro LM, Recio O, Duran P, J Mater Sci 30, 1931 (1995)
2. Navarro LM, Recio O, Duran P, J Mater Sci 30, 1939 (1995)
3. Navarro LM, Recio O, Duran P, J Mater Sci 30, 1949 (1995)
4. Choi SR, Bansal NP, Ceramics International 31, 39 (2005)
5. Feighery AJ, Irvine JTS, Solid State Ionics 121, 209 (1999)

SOFC Anode

1. Zhu WZ, Seevi SC, Mater Sci Eng A 362, 228 (2003)
2. Costamagna P, Costa P, Antonucci V, Electrochimica Acta 43, 375 (1998)
3. Uanner CW, Fung KZ, Virkar AV, J Electrochem Soc 144, 21 (1997)
4. Maier J, Nature Materials 4, 805 (2005)
5. Verweij H, Adv Mater 10, 1483 (1998)
6. de Boer B, Gonzalez M, Bouwmeester HJM, Verweij H, Solid State Ionics 127, 269 (2000)
7. Jiang SP, Chan SH, J Mater Sci 39, 4405 (2004)

SOFC Cathode

1. Fleig J, Annu Rev Mater Res 33, 361 (2003)
2. Fleig J, Maier J, J European Ceram Soc 24, 1343 (2004)
3. Chan SH, Chem XJ, Khor KA, J Electrochem Soc 151, A164 (2004)

References (cont'd)

SOFC Stability

1. Badwal SPS, Solid State Ionics 143, 39 (2001)
2. Lowrie FL, Rawlings RD, J European Ceram Soc 20, 751 (2000)
3. Montross CS, Yokokawa H, Dokiya M, British Ceramic Transactions 101, 85 (2002)
4. Haile SM, Acta Mater 51, 5981 (2003)

Thermoelectric Materials

1. Tritt TM, Subramanian MA, MRS Bulletin 31, 188 (2006)
2. Rao AM, Ji X, Tritt TM, MRS Bulletin 31, 218 (2006)
3. Yang R, Chem G, Phys Rev B 69, 195316 (2004)
4. Yang R, Chem G, Dresselhaus MS, Phys Rev B 72, 125418 (2005)
5. Zhao XB, Ji XH, Zhang YH, Zhu TJ, Tu JP, Zhang XB, Appl Phys Lett 86, 062111 (2005)
6. Tritt TM, eds., Thermal conductivity, Springer (2004)

References (cont'd)

Multiscale Theory

- Liu, W. K., and McVeigh, C. "Predictive Multiscale Theory for Design of Heterogeneous Materials." Computational Mechanics, 2007, DOI: 10.1007/s00466-007-0176-8.
- Cahal McVeigh, Franck Vernerey, Wing Kam Liu, Brian Moran, Gregory Olson. "An Interactive Microvoid Shear Localization Mechanism in High Strength Steels", *Journal of the Mechanics and Physics of Solids*, 55(2):225-224, 2007
- Vernerey F.J, Liu W.K, and Moran B. Multi-scale Micromorphic Theory for Hierarchical Materials. J. Mech. Phys. Solids. doi:10.1016/j.jmps.2007.04.008.
- Cahal McVeigh, Franck Vernerey, Wing Kam Liu and L. Cate Brinson. "Multiresolution analysis for material design". *Computer Methods in Applied Mechanics and Engineering*, 195(37-40):5053-5076, 2006.
- Liu, W. K., Karpov, E., and Park, H. S., *Nano Mechanics and Materials: Theory, Multiscale Methods and Applications*, Wiley, 2005.
- Park HS, Karpov EG, Klein PA, Liu WK, Three-Dimensional Bridging Scale Analysis of Dynamic Fracture. *Journal of Computational Physics* 207, 588-609, 2005
- W. K. Liu, E. Karpov, S. Zhang, and H. Park, "An Introduction to Computational Nano Mechanics and Materials," *Computer Method in Applied Mechanics and Engineering*, 193 (17-20): 1529-1578 2004.
- Li, S., and Liu, W. K., *Meshfree and Particle Methods*, Springer, (2004).
- Nemat-Nasser S., Hori M., Micromechanics: Overall Properties of Heterogeneous Materials, North Holland, 1999
- Vernerey F.J., McVeigh C., Liu W.K., Moran B., Tewari D., Parks D., Olson G. 3D Computational Modeling of Shear Dominated Ductile Failure of Steel, Journal of The Minerals, Metals and Materials Society, pp. 45-51, December 2006.
- Hao S., Liu W.K., Moran B., Vernerey F., and Olson G.B. Multiple-scale constitutive model and computational framework for the design of ultra-high strength, high toughness steels. Comput. Methods Appl. Mech. Engrg, 2004.